Direct Evidence of Torsional Motion in an Aggregation-Induced Emissive Chromophore

ARTICLE *in* THE JOURNAL OF PHYSICAL CHEMISTRY C · DECEMBER 2013

Impact Factor: 4.77 · DOI: 10.1021/jp4104504

5 AUTHORS, INCLUDING:

Tersilla Virgili
Italian National Research Council
78 PUBLICATIONS **1,433** CITATIONS
SEE PROFILE

Alessandra Forni
Italian National Research Council
109 PUBLICATIONS **1,500** CITATIONS
SEE PROFILE

Dario Pasini
University of Pavia
94 PUBLICATIONS **1,210** CITATIONS
SEE PROFILE

Chiara Botta
Italian National Research Council
193 PUBLICATIONS **2,011** CITATIONS
SEE PROFILE

THE JOURNAL OF PHYSICAL CHEMISTRY C

Article

pubs.acs.org/JPCC

Direct Evidence of Torsional Motion in an Aggregation-Induced Emissive Chromophore

Tersilla Virgili,*[,†] Alessandra Forni,*[,‡] Elena Cariati,[§] Dario Pasini,[∥] and Chiara Botta[⊥]

[†]Istituto di Fotonica e Nanotecnologie (IFN)-CNR, Dipartimento di Fisica, Politecnico di Milano, P.zza Leonardo Da Vinci 32, 20132 Milano, Italy

[‡]ISTM-CNR, Institute of Molecular Sciences and Technologies of CNR, via Golgi 19, 20133 Milano, Italy

[§]Dipartimento di Chimica dell'Università degli Studi di Milano, UdR del INSTM di Milano,via Golgi 19, 20133 Milano, Italy

[∥]Department of Chemistry and INSTM Research Unit, University of Pavia, Viale Taramelli, 10-27100 Pavia, Italy

[⊥]Istituto per lo Studio delle Macromolecole (ISMAC), CNR, Via Bassini 15, 20133 Milano, Italy

Supporting Information

ABSTRACT: The aggregation induced emission (AIE) behavior shown by organic chromophores is very interesting for the development of efficient solid state devices. The restriction of intramolecular rotation is by far the most frequently assumed mechanism to explain this behavior; by blocking or reducing this rotation, upon rigidification of the environment, molecular luminescence is restored. By means of ultrafast pump−probe spectroscopy combined with density functional theory (DFT) and time-dependent DFT calculations, we show direct evidence of intramolecular rotation in a simple push−pull organic chromophore,4-diethylamino-2 benzylidene malonic acid dimethyl ester, possessing AIE properties. The spectral evolution of the stimulated emission band of the chromophore in the first 45 ps after photoexcitation is fully consistent with the presence of a torsional relaxation toward the equilibrium geometry of the excited state, taking place on time scales that depend on the solvent viscosity. The structural features of the excited state fully account for the different photoluminescence efficiencies observed in solvents with different viscosities.

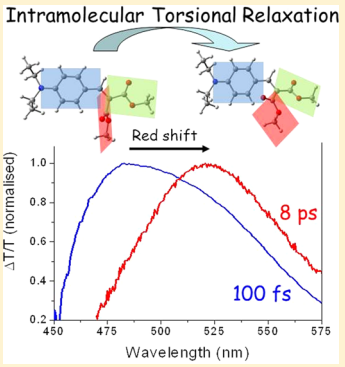

INTRODUCTION

Fluorescent dyes in which π-electrons are delocalized over extended molecular frameworks are of fundamental importance for a series of advanced technologies in the fields of optics and electronics.[1] In order to emit with high quantum yields, these molecules generally have to be isolated from each other (either in matrices/solutions at very low concentrations or in nanostructured host−guest systems) so that aggregation-caused emission quenching (ACQ), associated with the formation of less emissive species such as exciplexes and excimers, can be avoided.[2] A still limited number of organic chromophores have been recently found to emit more efficiently in the aggregated state than in solution.[3−5] This behavior, clearly very promising for the construction of efficient solid state devices such as light-emitting diodes, has been defined as aggregation-induced-emission (AIE) since the pioneering works of Tang and co-workers.[6] The restriction of intramolecular rotation (RIR) is by far the most frequently assumed mechanism to explain the AIE behavior.[3,6] In solution, the free intramolecular rotation introduces a nonradiative relaxation channel for the excited state to decay; by slowing or stopping this rotation, as a consequence of aggregation, molecular luminescence is restored. While deep studies have been reported on the low-frequency vibrational dynamics of prototypical systems, such as tetraphenylethylene,[7] in-depth photophysical studies on the role of intramolecular rotations in activating radiative/non-radiative recombination channels have not been fully addressed, in particular as far as chromophores showing AIE properties are concerned. Time-resolved fluorescence studies on tetraphenylethylene and silole derivatives assigned a posteriori their AIE properties to the deactivation in the aggregate form of nonradiative decays caused by intramolecular torsional motions.[8,9] Recently, we have reported a new family of simple molecular frameworks, namely, 4-dialkylamino-2-benzylidene malonic acid dialkyl esters, which possess interesting AIE properties.[10,11] Independently on the solvent polarizability, their weak emission (PLQY below 0.1%) in solution strongly increases either upon solvent rigidification (by increasing the solvent viscosity) or by lowering the temperature.

In this paper, we focus our attention on the conformational reorganization following photoexcitation of one of the previously investigated AIE molecules, 4-diethylamino-2 benzylidene malonic acid dimethyl ester (**1**), by means of ultrafast pump probe (P&P) spectroscopy and accurate density functional theory (DFT) and time-dependent DFT (TDDFT) calculations. The P&P technique, allowing to follow the excited-state dynamics after pump excitation, provides a direct measure of both radiative and nonradiative decay of the

Received: October 22, 2013
Revised: November 29, 2013

   dx.doi.org/10.1021/jp4104504 | J. Phys. Chem. C XXXX, XXX, XXX−XXX

molecule, the latter often mediated by vibrational, rotational, and torsional motions. By following the temporal evolution of the stimulated emission (SE), we show that the viscosity of the solvent slows down the torsional relaxation of the organic compound, determining a higher photoluminescence quantum yield (PLQY). Previous works using this or other time-resolved spectroscopic techniques to study torsional relaxation processes were limited to oligo- and polythiophenes and fluorene systems[12−17] that do not possess AIE properties. We show here a strong evidence, supported by accurate DFT and TDDFT calculations, of the picoseconds torsional motion bringing the AIE molecule from an initial emissive excited structure to a lower energy equilibrium geometry, rather different from the initial one and characterized by less efficient emission. We demonstrate how, by increasing the solvent viscosity, such torsional motion is slowed down, and consequently the process of internal conversion along the excited state becomes less efficient, accounting for the PLQY dependence on the viscosity of the solvents.

METHODS

Compound **1**, shown in the inset of Figure 1, was synthesized according to the literature.[10] The compound was dissolved in four different solvents: polyethylene glycol (PEG) with a molecular weight of 400, diethylene glycol (DEG), dichloromethane (DCM), and a acetonitrile (ACN) using a molar concentration of 10^{-5} for the PLQY measurements and of 10^{-3} for the P&P measurements.

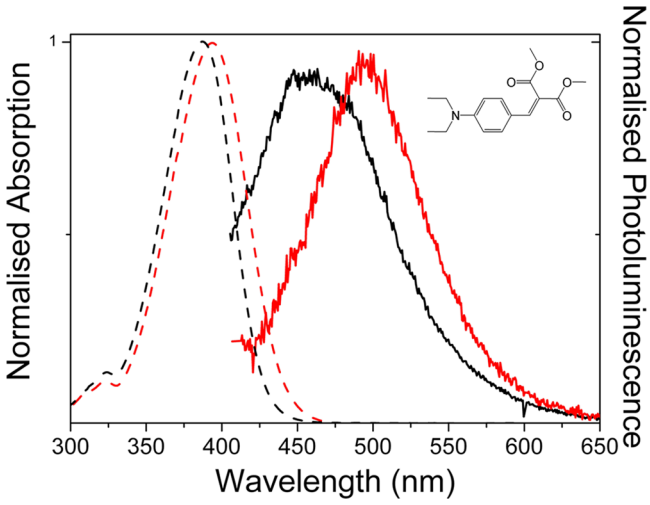

Figure 1. Absorption (dashed line) and emission (solid line) spectra for PEG (black line) and DEG (red line) solution. In the inset the chemical structure of **1** is shown.

Photoluminescence (PL) continuous wave measurements are obtained with a SPEX 270 M monochromator equipped with a N_2 cooled charge-coupled device exciting with a monochromated Xe lamp. The spectra are corrected for the instrument response. PLQYs are obtained by using quinine sulfate as a reference and exciting at 365 nm. The experimental error in the PLQYs is about 3% while no reliable values are reported below 0.001 due to the limit of the detection system.

In the femtosecond pump−probe transient absorption spectroscopy experiment,[18] pump pulses at 3.18 eV (390 nm) (second harmonic of the output of a CLARK Ti:sapphire regenerative amplifier with a repetition rate of 1 kHz and a pulse length of 150 fs) are focused to a spot of ∼150 μm diameter with an energy of excitation of 1.3 mJ/cm^2 The probe beam is a white light continuum 1.77−2.76 eV (450−700 nm), generated by focusing a small percentage of the CLARK amplifier output energy onto a sapphire plate. The pump and probe beams are spatially overlapped on the sample. The probe beam intensity used in the experiment is kept deliberately low. The evolution of the differential transmission ($\Delta T/T$) was recorded within the visible spectral range using a fast optical multichannel analyzer (OMA) as a detection system.

All calculations have been performed with the Gaussian suite of programs.[19] Geometry optimizations have been performed at the PBE0/6-311++G (d,p) level[20,21] for the ground state (S_0) and at the CAM-B3LYP/6-311++G (d,p) level[22] for the excited state (S1). Calculations were carried out in DCM using the conductor-like polarizable continuum model, CPCM,[23] according to two different approaches: the linear-response (LR) method[24] and the state-specific (SS) method.[25,26] The better agreement with the experimental emission spectra has been obtained with the LR approach and in the paper we report the results obtained within this method. The full body of the computational results is provided as Supporting Information. We denote by λ_{max}^{abs} the absorption maximum, corresponding to the vertical excitation energy from S_0 to S_1, and by λ_{max}^{em} the emission maximum, corresponding to the vertical emission energy from S_1 to S_0, at the end of the minimization process of S_1 (i.e., with the ground state at the geometry of the optimized excited state).

RESULTS AND DISCUSSION

Table 1 shows the main spectroscopic characteristics of compound **1** in different solvents. The PLQY of the solutions is not influenced by the solvent polarizability (DCM and ACN being the solutions with the lowest and highest polarizability, respectively); on the contrary the PL efficiency is strongly influenced by the viscosity of the solvent. Due to the extremely weak emission of **1** in ACN and DCM solutions, we focused our attention on the PEG and DEG solutions in order to investigate the role of solvent viscosity on the PL efficiency. Figure 1 shows the absorption (dashed line) and photoluminescence (solid line) spectra of **1** in PEG (black line) and in DEG (red line). We performed ultrafast pump−probe measurements on the two solutions in order to temporally resolve the spectral evolution of the excited states created after the pump excitation. In this experiment, the transmission of a white light pulse (probe) is detected at different time delays

Table 1. Optical Properties of Compound 1 Dissolved in Different Solvents

	λ_{abs} (nm)	λ_{em} (nm)	Stokes shift (eV)	orientation polarizability of the solvent (Δf)	viscosity of the solvent (cP)	PLQY
acetonitrile (ACN)	384	490	0.70	0.305	0.37	<0.001
dichloromethane (DCM)	386	480	0.607	0.220	0.44	<0.001
diethylene glycol (DEG)	394	494	0.637	0.266	35.7	0.003
polyethylene glycol (PEG)	388	453	0.459	0.225	90	0.026

dx.doi.org/10.1021/jp4104504 | J. Phys. Chem. C XXXX, XXX, XXX−XXX

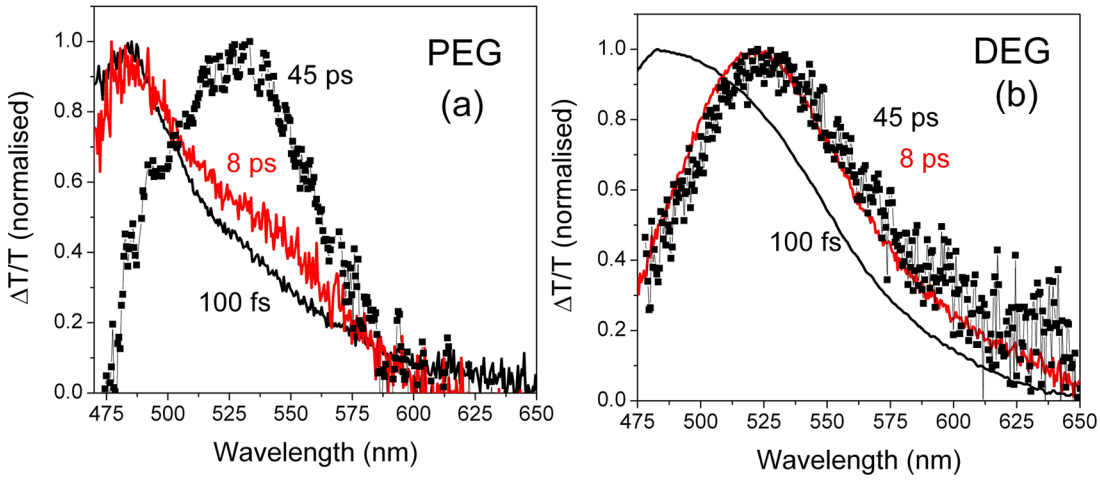

Figure 2. Differential transmission spectra at 100 fs (black line), at 8 ps (red line), and at 45 ps probe delay (line plus symbols) for PEG (a) and for DEG solution (b).

with respect to the pump excitation (390 nm). The differential transmission spectra of the probe pulse $\Delta T/T$ (where $\Delta T = T_{on} - T$, with T_{on} being the transmission of the probe light with the pump excitation and T being the transmission of the probe light without the pump excitation) taken at different probe delays is then obtained. Positive $\Delta T/T$ signal (transmission increasing after pump excitation) is an indication of bleaching of the ground state when the signal spectrally overlaps the absorption spectrum or of stimulated emission (SE) from the excited state when the signal overlaps the PL spectrum of the molecule.

Figure 2 shows $\Delta T/T$ spectra collected at different probe delays after pump excitation for the PEG (left side) and the DEG solutions (right side). The $\Delta T/T$ spectra at 100 fs probe delay (black line) are similar for both solutions. These spectra show a positive band peaked at around 480 nm assigned to SE. Such band, observed just after the pump excitation, corresponds to the instantaneous emission by the molecules. By increasing the probe time delay to 8 ps (see Figure 2b red line), the DEG solution shows a clear red shift (~170 meV) of the SE band that does not change its shape and position at longer probe time delay. Differently, for the PEG solution the $\Delta T/T$ spectrum changes more slowly. At 8 ps probe delay, a weak shoulder at 530 nm appears in the SE band (see red line in Figure 2 a) and only after 45 ps from the excitation the SE band presents a red shift as in the DEG solution (see Figure 2a, black line plus symbols). The redshift of the stimulated emission band can be connected with the shift of the spontaneous emission band and can be explained by an internal relaxation of the molecular geometry from the ground-state one toward the minimum-energy one of the excited state, the latter emitting at 530 nm. It can be hypothesized that such relaxation implies intramolecular rotation, which is expected to be slower and less probable in the more viscous solvent. This rotation increases the planarity of the molecule with respect to the ground state, in fact, a more extended conjugation framework can account for the large red shift observed in the stimulated and consequently in the spontaneous emission spectrum (see Figure 1).

The very low PLQY obtained in the less viscous DEG solution (and even lower in DCM and ACN, see Table 1), where relaxation occurs faster after excitation can be due to the fact that, as it will be discussed later, the relaxed geometry is less emissive than the ground state one. PLQY is higher in PEG because molecules can preserve their initial geometry for a longer time. To confirm this picture we analyzed the temporal decays of the signal at 530 nm (see Figure 3) by performing a

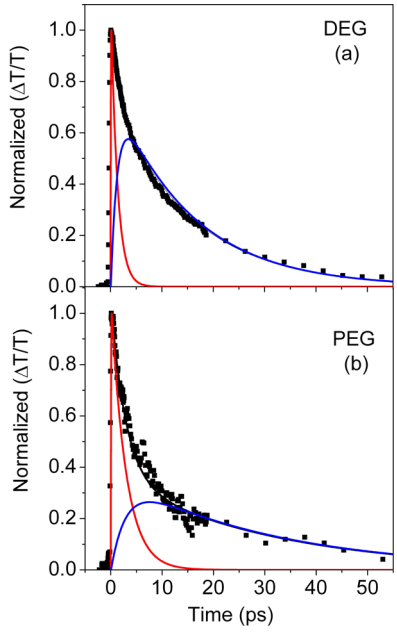

Figure 3. Experimental decay (black symbols) at 530 nm, theoretical fit (black line), $y(1)$ (red line), and $y(2)$ population decay (blue line) for the DEG (a) and PEG solution (b).

simple numerical fitting of the $\Delta T/T$ dynamics in the two solvents. We assumed that the signal at this wavelength for both solvents is the sum of two contributions. One is due to the population of molecules (emitting band peaked at ~480 nm) that have preserved the ground state conformation after the pump excitation, $y_1(t)$. The other corresponds to the population of the molecules (emitting band peaked at ~530 nm) that underwent the torsional relaxation, $y_2(t)$. The signal observed at 530 nm in the two solvents can be then ascribed to total populations PEG530 and DEG530 given respectively by

$$\text{PEG530} = y_1(t) + a.y_2(t) \quad (1)$$

dx.doi.org/10.1021/jp4104504 | J. Phys. Chem. C XXXX, XXX, XXX−XXX

$$\mathrm{DEG530} = y_1(t) + a^{*}y_2(t) \quad (2)$$

where a is the relative contribution of $y_2(t)$ to the total signal. By assuming that $y_1(t)$ population either relaxes radiatively or undergoes nonradiative torsional relaxation toward the "planar" conformation $y_2(t)$, the dynamics of the two populations is described by the following rate equations

$$\frac{dy_1(t)}{dt} = G(U) - (k_1^{NR} + k_1^{R}).\, y_1(t) \quad (3)$$

$$\frac{dy_2(t)}{dt} = k_1^{NR}.\, y_1(t) - k_2.\, y_2(t) \quad (4)$$

where $G(U)$ represents the population created with pump-pulse initial excitation, k_1^{NR} is the nonradiative decay rate constant of $y_1(t)$, k_1^{R} is the radiative one, and k_2 is the decay rate constant of $y_2(t)$. Figure 3 shows the $\Delta T/T$ experimental decay (symbols) with the numerical fit (black solid line) of the two populations $y_1(t)$ (red line) and $y_2(t)$ (blue line) as obtained from the equations reported above.

In Table 2, we report the parameters obtained by the fitting procedure for the two solutions. Upon pump excitation, $y_1(t)$ is

Table 2. Parameters Resulted by the Fitting Procedure

	k_1^{NR}	k_1^{R}	k_2	a
PEG	$(4.5\ \mathrm{ps})^{-1}$	$(8\ \mathrm{ps})^{-1}$	$(30\ \mathrm{ps})^{-1}$	0.5
DEG	$(1.5\ \mathrm{ps})^{-1}$	$(8\ \mathrm{ps})^{-1}$	$(15\ \mathrm{ps})^{-1}$	0.8

created instantaneously by the pump excitation and decays radiatively with the same decay rate constant k_1^R, independently on the solvent. The nonradiative channel of $y_1(t)$ (k_1^{NR}), which transfers part of the $y_1(t)$ population to the $y_2(t)$, is faster for the less viscous DEG solution with respect to the PEG one. Finally, the $y_2(t)$ population of the relaxed molecules decays differently in the two solutions, being faster for the DEG solution. This suggests that both radiative and nonradiative decay channels come into play for $y_2(t)$ also. The a factor represents the ratio of relaxed molecules with respect to the nonrelaxed ones: the lower value of a for the PEG solution shows that the higher viscosity of this solution inhibits the intramolecular rotation while the latter is more probable in the DEG solution. It is necessary to underline the fact that this simple model is mainly qualitative but it allows one to envisage the different efficiencies of the torsional motion in the two solvents. Using this model it is also evident that the SE spectrum contains the contribution from both the emission of the nonrelaxed molecules population (PL peak at ~480 nm) and of the more planar molecules population (PL peak at ~530 nm).

A further proof of the consistency of this picture is given by PBE0/6-311++G** and TD-CAM-B3LYP/6-311++G** calculations on the ground and the excited states, respectively, starting from the experimental geometry as obtained by single crystal X-ray diffractometric studies.[10] Such calculations, allowing to determine the minimum-energy geometry of both states, have been performed in DCM, relying on the observation that at long probe delay the spectral position of the SE band coming from the relaxed molecules (see line plus symbols in Figure 2a,b) is the same, independently on the solvent and in particular on its viscosity. Our calculations provided a λ_{max}^{abs} value of 357 nm, which is in reasonable agreement with the experimental value (see Table 1), with the difference being between the two results in the range of the generally accepted error (0.3 eV) associated with TDDFT calculations. The $S_0 \rightarrow S_1$ vertical transition mainly corresponds to a $\pi \rightarrow \pi^*$ excitation from the highest occupied molecular orbital to the lowest unoccupied molecular orbital (HOMO→LUMO excitation). It is a very intense transition (oscillator strength f = 1.3) and it is associated with a slight increase (about 7 D) of the dipole moment, denoting a charge-transfer character of the transition as evidenced also by a weak solvatochromism (see Table S1 in Supporting Information for calculations in other solvents). Geometry optimization of the S_1 state allowed to obtain the equilibrium geometry of the excited state. The computed value of λ_{max}^{em}, 478 nm, should correspond in our model to the emission by the $y_2(t)$ population. This value underestimates (by 0.25 eV) the experimental one found with the P&P experiments, being in this case ~530 nm. However, if we compare the computed Stokes shift (0.88 eV) with the experimental one (0.86 eV) we can note a very good agreement. Geometry relaxation of the S_1 state toward the minimum implies a reduction of the excited state dipole moment, so that the difference between excited and ground state dipoles drops to about 4 D. The computed variations of the dipole moment in absorption and emission are in reasonable agreement with that experimentally determined for the analogous derivative with the dimethylamino instead of diethylamino group, which amounted to about 5 D.[10] Finally, it is important to note that the oscillator strength of the $S_1 \rightarrow S_0$ transition, f = 0.96, is significantly lower (by about 30%) than that of the $S_0 \rightarrow S_1$ transition, which can be assumed to be the oscillator strength of the vertical emission by the unrelaxed excited molecules. This result is in agreement with both the low PLQY observed in the experimental spectra in the nonviscous solvents and with the slight blueshift found in the PL spectrum of the PEG solution, characterized by the higher PLQY (see Table 1 and Figure 1, blue line). Because the PL spectrum shown in Figure 1 is a time integrated measurement, most of the signal comes from the longer living emitting species and from the more efficient one. In this case, the most efficient one is $y_1(t)$, but the radiative decay of this population competes with the internal conversion (nonradiative decay) that leads to the formation of the less efficient $y_2(t)$ population. In PEG solution, this nonradiative decay is less competitive, leading not only to a higher PLQY, but also to a slight blue shift of the spontaneous emission.

The S_0- and S_1-optimized structures are shown in Figure 4. It is well evident that the molecule undergoes a significant conformational rearrangement in the excited state on going from the S_0 to the S_1 relaxed geometry. The most evident geometrical variation is observed in the relative disposition of

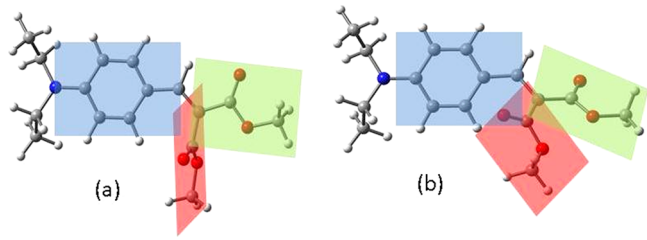

Figure 4. Optimized structures of the ground state at the PBE0/6-311++G** level of theory (a, left) and of the first excited singlet state at the CAM-B3LYP/6-311++G** level of theory (b, right) of the compound in dichloromethane.

dx.doi.org/10.1021/jp4104504 | J. Phys. Chem. C XXXX, XXX, XXX−XXX

the ester groups with respect to both each other and the aryl moiety, as evidenced by looking at the dihedral angles ϕ between the least-squares planes through the respective heavy atoms (drawn in blue, red, and green in Figure 4 for the aryl and the two ester groups, respectively). In the ground state (Figure 4a, left), the two ester groups (red and green planes) are almost perpendicular to each other (ϕ_1 = 88°) with one of them (green plane) essentially in the plane of the benzene ring (ϕ_2 = 2°), showing significant conjugation degree with it compared with the other ester group. Such minimum energy conformation compares well with the X-ray one[10] as far as the relative disposition of the ester groups is concerned ($\phi_{1,exp}$ = 81.0(1)°), while, as a consequence of crystal packing effects, a greater dihedral angle is observed between benzene and the most conjugated ester group ($\phi_{2,exp}$ = 32.0(1)°). On the contrary, in the S_1 optimized state (Figure 4b, right) the ester groups approach a coplanar conformation (ϕ_1 = 33°), becoming very similar in geometry and undergoing a rotation with respect to the benzene ring (ϕ_2 = 44 and 56°, respectively, for the green and red planes). As a result, in the S_1 state conjugation is extended to a larger portion of the molecule, including both the ester groups together with the benzene ring. In all cases (experimental geometry and theoretical S_0 and S_1 geometries), the atoms are in the considered planes within 0.02 Å. Other remarkable differences between the S_0 and S_1 states are observed in the bond distances (see Table S2 in Supporting Information for a detailed comparison), clearly denoting for the aryl moiety a change from an aromatic to a quinoidal structure. For example, the single and double bonds connecting benzene with the malonate group shorten and lengthen, respectively, by 0.03 and 0.07 Å on going from S_0 to S_1.

CONCLUSIONS

In conclusion, by means of combined ultrafast pump−probe spectroscopy, and accurate quantum-mechanical calculations, we shine light on the mechanism of intramolecular rotation generally assumed to be responsible for AIE properties. Pump−probe experiments evidence the presence of a dynamic relaxation process in the excited state of the molecule, consisting in a conformational rearrangement of its functional groups with respect to the geometry assumed in the ground state, leading the molecule to a less emissive state. Such relaxation, as predicted by DFT and TDDFT calculations, consists in a concerted torsional motion bringing the molecule to a more planar conformation, whose structure is closer to a quinoidal rather than an aromatic system. We show that this conformational rearrangement occurs with a rate of 1.5 ps^{-1} in a solvent (DEG) with moderate viscosity, while in a more viscous solvent (PEG) the rate becomes slower ((4.5 ps^{-1}). From the analysis of the stimulated emission dynamics, we infer the presence of two emissive populations: the first one, instantaneously generated upon photoexcitation, emits more efficiently at around 480 nm; the second one, generated after internal conversion, emits less efficiently at around 530 nm. The different contributions of the two populations account for the PL efficiences observed in the two solvents.

ASSOCIATED CONTENT

Supporting Information

Computational details of the DFT and TDDFT simulations. This material is available free of charge via the Internet at http://pubs.acs.org.

AUTHOR INFORMATION

Corresponding Authors

*(T.V.) E-mail: tersilla.virgili@polimi.it. Phone: +39-02-23996076.

*(A.F.) E-mail: alessandra.forni@istm.cnr.it. Phone: +39-02-50314273.

Notes

The authors declare no competing financial interest.

ACKNOWLEDGMENTS

A.F. acknowledges the CINECA Award N. HP10BFJG1H "IscrB-HEChro", 2011, for the availability of high-performance computing resources and support. Partial support by the University of Pavia, the CARIPLO Foundation (2006: "Self-Assembled Nanostructured Materials: A Strategy for the Control of Electrooptic Properties", E.C.; D.P., and A.F.), MIUR PRIN 2009A5Y3N9 (D.P.), INSTM-Regione Lombardia 2013 (D.P.) is gratefully acknowledged. The authors thank Sai Kiran Rajendran for help in the P&P experimental setup.

REFERENCES

(1) Howard, E. K.; Huang, J. Thin-Film Organic Electronic Devices. *Annu. Rev. Mater. Res.* **2009**, *39*, 71−92.

(2) Valeur, B.; Berberan-Santos, M. N. *Molecular Fluorescence*; Wiley-VCH Verlag & Co: Weinheim, Germany, 2012.

(3) Hong, Y.; Lam, J. W. Y.; Tang, B. Z. Aggregation-Induced Emission. *Chem. Soc. Rev.* **2011**, *40*, 5361−5388.

(4) Hong, Y.; Lam, J. W. Y.; Tang, B. Z. Aggregation-Induced Emission: Phenomenon, Mechanism and Applications. *Chem. Commun.* **2009**, 4332−4353.

(5) Yuan, W. Z.; Gong, Y.; Chen, S.; Yuan Shen, X.; Lam, J. W. Y.; Lu, P.; Lu, Y.; Wang, Z.; Hu, R.; Xie, N.; et al. Efficient Solid Emitters with Aggregation-Induced Emission and Intramolecular Charge Transfer Characteristics: Molecular Design, Synthesis, Photophysical Behaviors, and OLED Application. *Chem. Mater.* **2012**, *24*, 1518−1528.

(6) Luo, J.; Xie, Z.; Lam, J. W. Y.; Cheng, L.; Chen, H.; Qiu, C.; Sing Kwok, H.; Zhan, X.; Liu, Y.; Zhu, D.; et al. Aggregation-Induced Emission of 1-methyl-1,2,3,4,5-pentaphenylsilole. *Chem. Commun.* **2001**, 1740−1741.

(7) Shustova, N. B.; Ong, T.-C.; Cozzolino, A. F.; Michaelis, V. K.; Griffin, R. G.; Dincă, M. Phenyl Ring Dynamics in a Tetraphenylethylene-Bridged Metal−Organic Framework: Implications for the Mechanism of Aggregation-Induced Emission. *J. Am. Chem. Soc.* **2012**, *134*, 15061−15070.

(8) Ren, Y.; Lam, J. W. Y.; Dong, Y. Q.; Tang, B. Z.; Wong, K. S. Enhanced Emission Efficiency and Excited State Lifetime Due to Restricted Intramolecular Motion in Silole Aggregates. *J. Phys. Chem. B* **2005**, *109*, 1135−1140.

(9) Ren, Y.; Dong, Y. Q.; Lam, J. W. Y.; Tang, B. Z.; Wong, K. S. Studies on the Aggregation-Induced Emission of Silole Film and Crystal by Time-Resolved Fluorescence Technique. *Chem. Phys. Lett.* **2005**, *402*, 468−473.

(10) Cariati, E.; Lanzeni, V.; Tordin, E.; Ugo, R.; Botta, C.; Giacometti Schieroni, A.; Sironi, A.; Pasini, D. Efficient Crystallization Induced Emissive Materials Based on a Simple Push−Pull Molecular Structure. *Phys. Chem. Chem. Phys.* **2011**, *13*, 18005−18014.

(11) Coluccini, C.; Sharma, A. K.; Caricato, M.; Sironi, A.; Cariati, E.; Righetto, S.; Tordin, E.; Botta, C.; Forni, A.; Pasini, D. Switching of Emissive and NLO Properties in Push-Pull Chromophores with Crescent PPV-like Structures. *Phys. Chem. Chem. Phys.* **2013**, *15*, 1666−1674.

(12) Lanzani, G.; Nisoli, M.; De Silvestri, S.; Tubino, R. Femtosecond Vibrational and Torsional Energy Redistribution in Photoexcited Oligothiophenes. *Chem. Phys. Lett.* **1996**, *251*, 339−345.

(13) Hintschich, S. I.; Dias, F. B.; Monkman, A. P. Dynamics of Conformational Relaxation in Photoexcited Oligofluorenes and Polyfluorene. *Phys. Rev. B* **2006**, *74*, 045210−045220.
(14) Justino, L. L. G.; Ramos, M. L.; Abreu, P. E.; Carvalho, R. A.; Sobral, A. J. F. N.; Scherf, U.; Burrows, H. D. Conformational Studies of Poly(9,9-dialkylfluorene)s in Solution using NMR Spectroscopy and Density Functional Theory Calculations. *J. Phys. Chem. B* **2009**, *113*, 11808−11821.
(15) Chen, H. L. Excited-State Backbone Twisting of Polyfluorene as Detected From Photothermal After-Effects. *J. Phys. Chem. B* **2009**, *113*, 8527−8531.
(16) Parkinson, P.; Muller, C.; Stingelin, N.; Johnston, M. B.; Herz, L. M. Role of Ultrafast Torsional Relaxation in the Emission From Polythiophene Aggregates. *J. Phys. Chem. Lett.* **2010**, *1*, 2788−2792.
(17) Clark, J.; Nelson, T.; Tretiak, S.; Cirmi, G.; Lanzani, G. Femtosecond Torsional Relaxation. *Nat. Phys.* **2012**, *8*, 225−231.
(18) Cabanillas-Gonzalez, J.; Virgili, T.; Lanzani, G.; Yeates, S.; Ariu, M.; Nelson, J.; Bradley, D. D. C. Photophysics of Charge Transfer in a Polyfluorene/Violanthrone Blend. *Phys. Rev. B* **2005**, *71*, 014211:1−8.
(19) Frisch, M. J.; Trucks, G. W.; Schlegel, H. B.; Scuseria, G. E.; Robb, M. A.; Cheeseman, J. R.; Scalmani, G.; Barone, V.; Mennucci, B.; Petersson, G. A.; et al. *Gaussian 09*, Revision C.01; Gaussian, Inc.: Wallingford, CT, 2011.
(20) Ernzerhof, M.; Scuseria, G. E. Assessment of the Perdew-Burke-Ernzerhof Exchange-Correlation Functional. *J. Chem. Phys.* **1999**, *110*, 5029−5036.
(21) Adamo, C.; Barone, V. Toward Reliable Density Functional Methods Without Adjustable Parameters: The PBE0Model. *J. Chem. Phys.* **1999**, *110*, 6158−6170.
(22) Yanai, T.; Tew, D. P.; Handy, N. C. A New Hybrid Exchange-Correlation Functional Using the Coulomb-Attenuating Method (CAM-B3LYP). *Chem. Phys. Lett.* **2004**, *393*, 51−57.
(23) Barone, V.; Cossi, M. Quantum Calculation of Molecular Energies and Energy Gradients in Solution by a Conductor Solvent Model. *J. Phys. Chem. A* **1998**, *102*, 1995−2001.
(24) Scalmani, G.; Frisch, M. J.; Mennucci, B.; Tomasi, J.; Cammi, R.; Barone, V. Geometries and Properties of Excited States in the Gas Phase and in Solution: Theory and Application of a Time-Dependent Density Functional Theory Polarizable Continuum Model. *Chem. Phys.* **2006**, *124*, 094107−094115.
(25) Improta, R.; Barone, V.; Scalmani, G.; Frisch, M. J. A State-Specific Polarizable Continuum Model Time Dependent Density Functional Method for Excited State Calculations in Solution. *J. Chem. Phys.* **2006**, *125*, 054103:1−9.
(26) Improta, R.; Scalmani, G.; Frisch, M. J.; Barone, V. Toward Effective and Reliable Fluorescence Energies in Solution by a New State Specific Polarizable Continuum Model Time Dependent Density Functional Theory Approach. *J. Chem. Phys.* **2007**, *127*, 074504:1−9.